Received: 1 July 2022 | Revised: 28 August 2022 | Accepted: 6 September 2022

DOI: 10.1111/cas.15580

Cancer Science WILEY

ORIGINAL ARTICLE

# Targeting the PTP1B-Bcr-Abl1 interaction for the degradation of T315I mutant Bcr-Abl1 in chronic myeloid leukemia

Ahmed Elgehama[1] | Yixuan Wang[1] | Ying Yu[1] | Lin Zhou[1] | Zhixiu Chen[1] | Liwei Wang[1] | Lijun Sun[2] | Jian Gao[1] | Biao Yu[3] | Yan Shen[1] | Qiang Xu[1]

[1]State Key Laboratory of Pharmaceutical Biotechnology, School of Life Sciences, Nanjing University, Nanjing, China

[2]Department of Chemistry, University of Science and Technology of China, Hefei, China

[3]State Key Laborary of Bio-organic and Natural Products Chemistry, Shanghai Institute of Organic Academy, Shanghai, China

**Correspondence**
Yan Shen and Qiang Xu, State Key Laboratory of Pharmaceutical Biotechnology, School of Life Sciences, Nanjing University, Nanjing 210023, China.
Emails: shenyan@nju.edu.cn (YS); molpharm@163.com (QX)

**Funding information**
National Natural Science Foundation of China, Grant/Award Number: 21937005 and 81974504; Natural Science Foundation of Jiangsu Province, Grant/Award Number: BK20191251 and BK20210184

## Abstract

Small-molecule-induced degradation of mutant Bcr-Abl1 provides a potential approach to overcome Bcr-Abl1 tyrosine kinase inhibitor (TKI)-resistant chronic myeloid leukemia (CML). Our previous study reported that a synthetic steroidal glycoside SBF-1 showed remarkable anti-CML activity by inducing the degradation of native Bcr-Abl1 protein. Here, we observed the comparable growth inhibition for SBF-1 in CML cells harboring T315I mutant Bcr-Abl1 in vitro and in vivo. SBF-1 triggered its degradation through disrupting the interaction between protein-tyrosine phosphatase 1B (PTP1B) and Bcr-Abl1. Using SBF-1 as a tool, we found that Tyr46 in the PTP1B catalytic domain and Tyr852 in the Bcr-Abl1 pleckstrin-homology (PH) domain are critical for their interaction. Moreover, the phosphorylation of Tyr1086 within the Bcr-Abl1 SH2 domain recruited the E3 ubiquitin ligase c-Cbl to catalyze K27-linked ubiquitin chains, which serve as a recognition signal for p62-dependent autophagic degradation. PTP1B dephosphorylated Bcr-Abl1 at Tyr1086 and prevented the recruitment of c-Cbl, leading to the stability of Bcr-Abl1. This study unravels the action mechanism of PTP1B in stabilizing Bcr-Abl1 protein and indicates that the PTP1B-Bcr-Abl1 interaction might be one of druggable targets for TKI-resistant CML with point mutations.

**KEYWORDS**
Bcr-Abl1, chronic myeloid leukemia, PTP1B, SBF-1, T315I mutant

## 1 | INTRODUCTION

Chronic myeloid leukemia (CML) is a myeloproliferative disorder characterized by a fusion oncogene *Bcr-Abl1*.[1] The chimeric Bcr-Abl1 protein is a constitutively active tyrosine kinase that drives uncontrolled cellular proliferation through downstream signaling pathways that involve STAT5, MAPKs and PI3K.[2,3] Outcomes for patients with CML have been greatly improved by the development of Bcr-Abl1 tyrosine kinase inhibitors (TKIs) in the clinic, which becomes a translation paradigm initially paved by imatinib.[4] All Bcr-Abl1 TKIs currently target its adenosine triphosphate-binding site.[5] However, increasing cases have shown primary or acquired resistance, which is commonly caused by point mutations within the Bcr-Abl1 kinase domain.[6,7] Despite the appearance of second- and third-generation

Ahmed Elgehama and Yixuan Wang contributed equally to this work.

TKIs that provide effective control of point mutation-mediated resistance, therapy options are limited for patients with multiple Bcr-Abl1 mutations.[8]

Apart from inhibition of Bcr-Abl1 kinase activity, an alternative approach to treat CML is to degrade the Bcr-Abl1 protein. Several potent degraders against Bcr-Abl1 have been developed using protein knockdown technologies, such as proteolysis targeting chimeras (PROTACs) and specific and nongenetic inhibitor of apoptosis protein (IAP)-dependent protein erasers (SNIPERs). These degraders target Bcr-Abl1 protein and concomitantly recruit the proteasomal degradation system via bifunctional hybrid molecules.[9–11] The degradation of Bcr-Abl1 protein enables growth inhibition of CML cells harboring native or mutant forms, and even causes the eradication of CML stem cells.[11] A recent study has demonstrated that a short-term treatment of Bcr-Abl1 degrader shows more sustained inhibition of CML cell growth than Bcr-Abl1 kinase inhibitors, implying the clinic advantage of drug discontinuation.[12] Notwithstanding the success of Bcr-Abl1 degraders, the effectiveness of these hybrid molecules is still hampered by low cell permeability and micromolar potency.[13]

Protein-tyrosine phosphatase 1B (PTP1B) is required for the stabilization of Bcr-Abl1.[14,15] Inhibition of PTP1B activity via either pharmacological or small interfering RNA (siRNA) means mediates ubiquitination and degradation of Bcr-Abl1 protein.[14] Our previous study demonstrated that a synthetic steroidal glycoside SBF-1 can induce the degradation of native Bcr-Abl1 protein through disrupting the interaction between PTP1B and Bcr-Abl1 at nanomolecular levels.[15] Herein, we further explore the efficacy of targeting the PTP1B-Bcr-Abl1 interaction against imatinib-resistant Bcr-Abl1 mutants and unravel the underlying mechanisms for Bcr-Abl1 degradation.

## 2 | MATERIALS AND METHOD

### 2.1 | Chemicals, reagents, and antibodies

SBF-1 is a synthetic steroidal glycoside, as described previously.[15,16] Anti-c-Abl, anti-p-Bcr, anti-p-STAT5, anti-STAT5, anti-p-SHP-2, anti-c-Cbl, anti-HA-tag, anti-myc-tag, and anti-Beclin 1 antibodies were purchased from Cell Signaling Technology. Anti-SHP-2, anti-GAPDH, anti-PTP1B, and anti- ubiquitin antibodies were from Santa Cruz Biotechnology. Anti-p62, anti-ATG5, and anti-phosphotyrosine antibodies were from Abcam. MG132 and bafilomycin A1 (Baf A1) were from Selleck Chemicals. Anti-Flag-tag antibody, 3-(4,5-dimethylthiazol-2-yl)-2,5-diphenyltetrazolium bromide (MTT), imatinib, 3-Methyladenine (3-MA), chloroquine (CQ), 4′,6-diamidino-2-phenylindole (DAPI), and Oridonin were from Sigma-Aldrich. The lysosome-specific dye LysoTraker Red, Lipofectamine™ LTX Reagent, Lipofectamine 2000, and Lipofectamine RNAi MAX were from Life Technologies. SuperSep Phos-tag™ was from Wako. The RediPlate 96 EnzChek Tyrosine Phosphatase Assay Kit was from Thermo Fisher Scientific.

### 2.2 | Cell culture

Human CML cell lines K562 and K562/G were obtained from the Institute of Hematology, Chinese Academy of Medical Sciences. Ba-F3 cell lines harboring either wild type (WT; Ba-F3p210) or T315 mutation (Ba-F3T315I) of Bcr-Abl1 were kindly presented by Professor Yijun Chen (China Pharmaceutical University). The HEK293 cells were obtained from the Shanghai Institute of Cell Biology. These cells were maintained in RPMI-1640 or DMEM medium supplemented with 10% FBS, 100 U/ml penicillin, and 100 mg/ml streptomycin.

### 2.3 | Plasmids and siRNAs

Bcr-Abl1 p210 WT, PTP1B WT, HA-tagged ubiquitin and its mutant plasmids were purchased from Addgene. HA-PTP1B$_{WT}$, HA-PTP1B$_{Multi}$, HA-PTP1B$_{Y46T}$, HA-PTP1B$_{K116R}$, HA-PTP1B$_{D181E}$, HA-PTP1B$_{Q262N}$, GFP-PTP1B$_{WT}$, GFP-PTP1B$_{Y46T}$, Flag-Bcr-Abl1$_{WT}$, Flag-Bcr-Abl1$_{\Delta OD}$, Flag-Bcr-Abl1$_{\Delta PH}$, Flag-Bcr-Abl1$_{\Delta SH3}$, Flag-Bcr-Abl1$_{\Delta SH2}$, Flag-Bcr-Abl1$_{\Delta KD}$, Flag-Bcr-Abl1$_{Y852A}$, Flag-Bcr-Abl1$_{Y1086A}$, EYFP-Bcr-Abl1$_{WT}$, EYFP-Bcr-Abl1$_{Y852A}$, ECFP-PTP1B$_{WT}$, and ECFP-PTP1B$_{Y46T}$ were obtained by PCR-based mutation and amplification of the WT expression vector. Bcr-Abl1$_{T315I}$ plasmid was kindly presented by Professor Xia Li (The Fourth Military Medical University, China). siRNA were from Gene Script. Sequences of siRNAs are listed in Table S1.

### 2.4 | Cell viability assay

Cell viability was assessed using MTT assays as described previously.[15]

### 2.5 | Western blot, immunoprecipitation, and immunofluorescence analysis

Western blot analysis, immunoprecipitation, and immunofluorescence analysis were performed as previously described.[17] The densitometry of immunoblots was quantified with Image J software.

### 2.6 | In vivo murine CML models

The murine CML model was established through intravenous injection of Ba-F3 cells into Balb/c mice. Each male Balb/c mouse was injected with $3\times10^6$ Ba-F3p210 or Ba-F3T315I via the tail vein. Four weeks after the injection, an obvious increase in the numbers of leukemic cells in the peripheral blood and splenomegaly was observed. The CML mice ($n = 10$ each group) were administered with PBS, imatinib (50 mg/kg/day, oral gavage) or SBF-1 (5 μg/kg/day, intraperitoneal injection) for 2 weeks.

### 2.7 | Molecular docking

The initial three-dimensional geometric coordinates of the X-ray crystal structures of PTP1B (PDB ID: 1A5Y) and Bcr-Abl1 PH domain (PDB ID: 5OC7) were downloaded from the Protein Data Bank. Using AutoDock 4.2, Discovery studio 3.0, and SchrÖdinger Maestro molecular modeling software, the models of SBF-1 and/or the PH domain with PTP1B were processed using default settings, and the model with the lowest estimated free energy for binding was selected.

### 2.8 | Acceptor photobleaching-based quantitative FRET

HEK293 cells transfected with enhanced cyan fluorescent protein (ECFP)-PTP1B$_{WT}$, ECFP-PTP1B$_{Y46T}$, enhanced yellow fluorescent protein (EYFP)-Bcr-Abl1$_{WT}$ or EYFP-Bcr-Abl1$_{Y852A}$ plasmids were maintained in phenol red-free medium during imaging. Fluorescence resonance energy transfer (FRET) images were acquired on a Nikon C1 Laser Scanning Confocal Microscope. Acceptor photobleaching was performed using Nikon EZ-C1 software (Ver3.80). The EYFP signal was set for bleaching to 30% of the original intensity. The FRET efficiency (FRET$_{eff}$) was calculated using the following formula: $FRET_{eff} = (D_{post} - D_{pre})/D_{post}$, where $D_{post}$ is the fluorescence intensity of the donor (ECFP) after acceptor photobleaching and $D_{pre}$ is the fluorescence intensity of the donor before acceptor photobleaching. The FRET efficiency was considered as positive when $D_{post} > D_{pre}$.

### 2.9 | Microscale thermophoresis

The binding affinity of SBF-1 to PTP1B$_{WT}$ or PTP1B$_{Y46T}$ was determined by microscale thermophoresis (MST) as described previously.[18] Briefly, $1 \times 10^7$ HEK293 cells transfected with GFP-tagged PTP1B or free GFP plasmids were lysed in lysis buffer. Cell lysates were diluted in buffer A (50 mM Hepes buffer [PH7.5], 5 mM DTT, 10 mM $CaCl_2$, 50 mM NaCl and 0.05% Tween-20) to a final concentration at which the fluorescent signals of the GFP proteins were similar and above the detection limit of the Monolith NT.115 instrument. Next, 10 µl of the cell lysate was mixed with 10 µl of SBF-1 at various concentrations from 100 µM to 3.05 nM in buffer A containing 0.5% DMSO. Then, the mixture solutions were loaded into NT.115 standard coated capillaries and MST measurement was performed at 25°C, 80% LED power, and 10% IR-laser power. The *Kd* was calculated by fitting a standard binding curve to the average of three independent dilution series.

### 2.10 | Cellular thermal shift assay

For Cellular thermal shift assay (CETSA) with cell lysates,[19] HEK293 cells transfected with indicated plasmids were lysed in lysis buffer. After centrifugation, an equal amount of lysates was incubated with 80 nM of SBF-1 for 12 h at 4°C and then heated for 4 min in a PCR machine at a designated temperature (44–80°C).

Soluble proteins, collected in the supernatant, were transferred into a new e-tube. An equal amount of proteins was loaded onto 7.5% SDS-PAGE gels and analyzed using c-Cbl and GAPDH antibody.

### 2.11 | Mass spectrometry

K562 cells were treated without or with 40 nM of SBF-1 for 12 h. The cell lysates were immunoprecipitated with the c-Abl specific antibody, then the c-Abl immunoprecipitation was separated with SDS-PAGE followed by Commassie Blue staining. The band corresponding to the molecular weight of Bcr-Abl1 (210 KD) was excised from the gel and tryptically digested. The resulting peptides were analyzed using the nanoLC-MS/MS system, which was performed by Applied Protein Technology. LC-MS/MS analysis was performed on a Q Exactive mass spectrometer.

### 2.12 | Statistical analysis

Data are expressed as the means ± SD. All statistical analyses were performed using the SPSS version 10.0 statistical software. $P < 0.05$ was considered significant.

## 3 | RESULTS

### 3.1 | The degradation of Bcr-Abl1 protein induced by SBF-1 suppresses the growth of CML cells harboring either native or T315I mutant Bcr-Abl1

Our previous study demonstrates that SBF-1 has remarkable anti-CML effects on K562 and its imatinib-resistant form K562/G cells, harboring no mutation within the Bcr-Abl1 kinase domain.[15] To further explore its anti-CML potential in the cells with Bcr-Abl1 mutants, we tested the cytotoxicity of SBF-1 in Ba-F3 cells expressing either WT or T315I mutant Bcr-Abl1. SBF-1 inhibited the proliferation of both cells with similar potency at the range of 29 to 34 nM for $IC_{50}$ values (Figure 1A). Ba-F3T315I cells were conspicuously resistant to imatinib. SBF-1 specifically reduced the protein levels of both WT and T315I Bcr-Abl1, but not native c-Abl or total STAT5 in a dose- and time-dependent manner (Figure 1B). When a time course experiment was performed to monitor Bcr-Abl1 degradation in the presence of cycloheximide, which inhibits protein synthesis, SBF-1 treatment accelerated degradation of both WT and T315I mutant Bcr-Abl1 (Figure 1C). Meanwhile, the phosphorylation levels of Bcr-Abl1 and its substrates downstream were decreased in a similar pattern. Next, we injected intravenously Balb/c mice with Ba-F3p210 or Ba-F3T315I cells. Four weeks after transplantation, the mice were treated daily with 5 µg/kg SBF-1 or 50 mg/kg imatinib for 14 days. Imatinib prolonged the survival of the Ba-F3p210-bearing mice, but

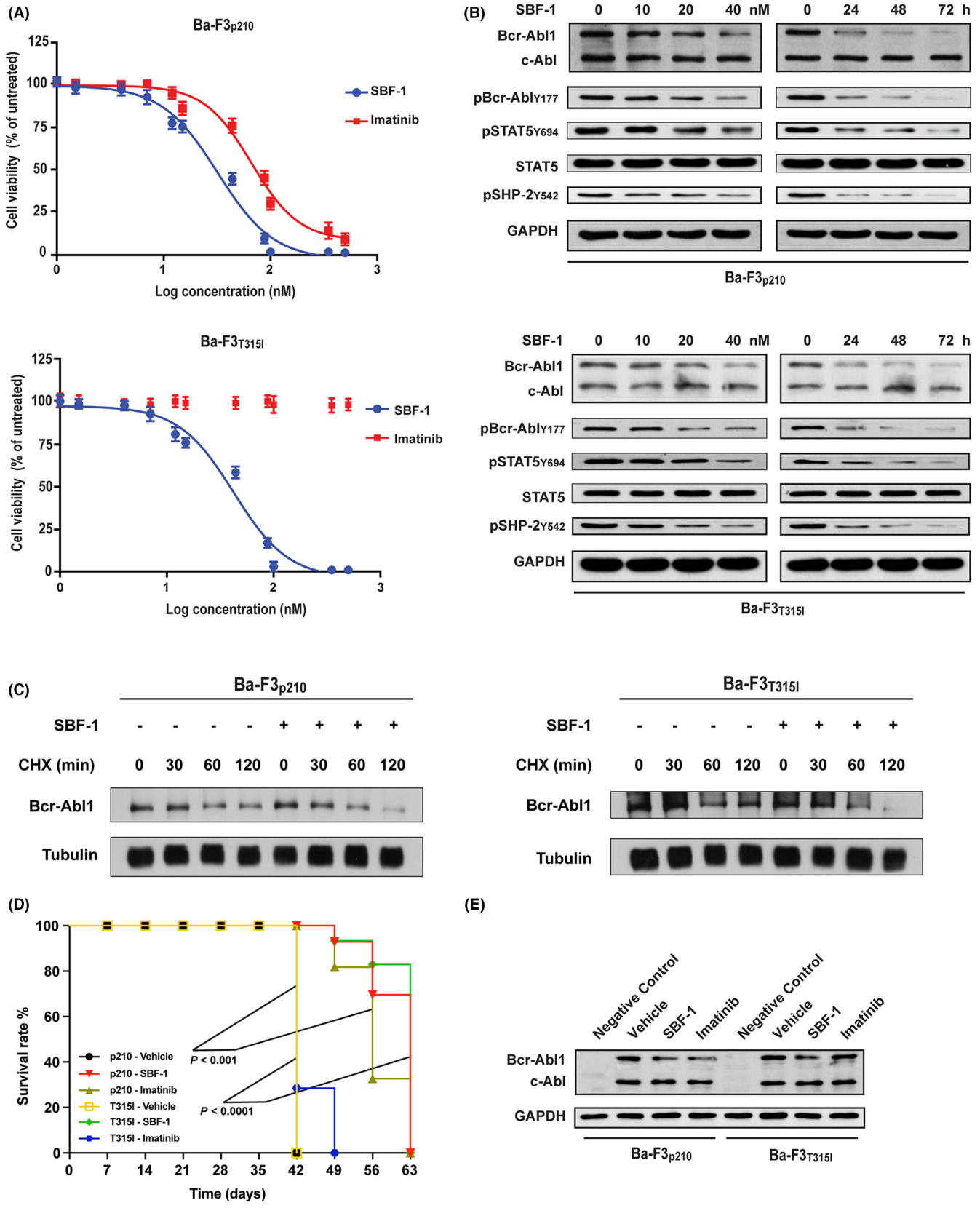


FIGURE 1 Growth inhibition of CML cells with either native or T315I mutant Bcr-Abl1 by SBF-1 through reducing Bcr-Abl1 protein. (A) Cell viability was determined by MTT assay when treated with SBF-1 for 72 h. (B) The expression of Bcr-Abl1 and its downstream signaling molecules were detected by western blot. (C) The degradation of Bcr-Abl1 over time in the presence of cycloheximide (CHX, 5 μg/ml) alone or in combination with SBF-1 (40 nM) was monitored by western blot. (D and E) Balb/c mice were injected with Ba-F3p210 or Ba-F3T315I cells via the tail vein. (D) Animal survival was monitored ($n = 10$). (E) Western blot analysis for Bcr-Abl1 protein expression in the blood samples isolated at day 40 post-transplantation

failed in Ba-F3T315I-bearing mice (Figure 1D). In contrast, SBF-1 prolonged the survival of both these leukemia cell-bearing mice with a significant survival advantage of 21 days over vehicle controls. Western blot analysis for the blood samples showed that SBF-1 treatment reduced Bcr-Abl1 protein expression in both Ba-F3p210- and Ba-F3T315I-bearing mice (Figure 1E).

### 3.2 | The blockade of the interaction between PTP1B and Bcr-Abl1 triggers the degradation of mutant Bcr-Abl1 protein

Given that PTP1B is required for the stability of Bcr-Abl1 and that SBF-1 is capable of directly blocking the interaction between PTP1B and native Bcr-Abl1,[14,15] we investigated whether PTP1B is also involved in the stability of mutant Bcr-Abl1. Silencing PTP1B with specific siRNA caused a reduction of Bcr-Abl1 protein in both imatinib-sensitive K562, Ba-F3p210 and imatinib-resistant K562/G, Ba-F3T315I cells (Figure 2A), and in turn inhibited the growth of these cell lines (Figure 2B). However, the cytotoxicity of SBF-1 was abolished by the knockdown of PTP1B in all these cells. Similar to our previous findings in K562 and K562/G cells,[15] the ubiquitination of Bcr-Abl1 immunoprecipitated from either Ba-F3p210 or Ba-F3T315I cell lysates was enhanced on SBF-1 treatment (Figure 2C). Immunoprecipitation assays revealed that SBF-1 disrupted the interaction between PTP1B and Bcr-Abl1 in both Ba-F3p210 and Ba-F3T315I cells, whereas imatinib did not (Figure 2D). Using the bone marrow samples from the Ba-F3p210 or Ba-F3T315I-bearing mice, we found that administering SBF-1, but not imatinib, disrupted the interaction of these two proteins (Figure 2E). Immunofluorescence analysis confirmed that SBF-1 impaired the co-localization of PTP1B with exogenous Bcr-Abl1$_{WT}$ and Bcr-Abl1$_{T315I}$ in HEK293 cells (Figure S1).

### 3.3 | Tyr46 in PTP1B and Tyr852 in Bcr-Abl1 PH domain are required for their interaction

To further explore the molecular basis of the PTP1B-Bcr-Abl1 interaction, we utilized SBF-1 as a tool and employed molecular docking to analyze the binding of SBF-1 to PTP1B protein. The model with the most favorable binding free energy and reasonable orientation was selected (Figure 3A). SBF-1 could form hydrogen bonds with residues Tyr46, Lys116, Asp181, and Gln262 within the PTP1B catalytic domain. We reasoned that these residues might be also crucial for the PTP1B-Bcr-Abl1 interaction, and thereby generated a multiple mimetic mutant of these four residues and their respective mutants. Immunoprecipitation assays showed that the Y46T mutation of PTP1B reduced the binding of Bcr-Abl1 the most (Figure 3B). In addition, the ubiquitination of Bcr-Abl1 was dramatically increased in cells co-transfected with the PTP1B Y46T mutant as compared with those with WT PTP1B (Figure 3C). Moreover, we employed single-cell acceptor photobleaching FRET using the two proteins tagged with the ECFP:EYFP fluorescent protein pair. The ECFP fluorescence was markedly enhanced after EYFP photobleaching in HEK293 cells co-transfected with ECFP-PTP1B$_{WT}$ and EYFP-Bcr-Abl1$_{WT}$ plasmids (Figure 3D). In the case of ECFP-PTP1B$_{Y46T}$, the intensity of ECFP fluorescence did not vary. The efficiency of FRET between ECFP-PTP1B$_{WT}$ and EYFP-Bcr-Abl1$_{WT}$ was much higher than that between ECFP-PTP1B$_{Y46T}$ and EYFP-Bcr-Abl1$_{WT}$ (Figure 3E). Similarly, the Y46T mutation in PTP1B abolished the binding of T315I Bcr-Abl1 and promoted its degradation (Figure 3F). Immunoprecipitation assays confirmed that, like WT Bcr-Abl1, T315I Bcr-Abl1 was specifically ubiquitinated after co-transfection with PTP1B$_{Y46T}$ (Figure 3G).

To understand which Bcr-Abl1 domain is involved in the binding with PTP1B, we conducted immunoprecipitation assays with several truncated forms of Bcr-Abl1. We observed that the truncation of Bcr-Abl1 PH domain abolished the binding of PTP1B, whereas deletion of other domains, including the N-terminal oligomerization domain (OD), the central SH3, SH2, as well as the kinase domain (KD), had little effect (Figure 4A). On the basis of these results, we performed modeling for the PTP1B-SBF-1-Bcr-Abl1 PH domain complex and found that several residues within the PH domain, such as Tyr852, are proximal to the position where SBF-1 binds to PTP1B (Figure 4B). In the predicted scenario of the complex, both Tyr46 in PTP1B and Tyr852 in the Bcr-Abl1 PH domain are possibly crucial for their interaction (Figures 4C and S2). Interestingly, the Y852A mutation in the Bcr-Abl1 PH domain exactly disrupted the PTP1B-Bcr-Abl1 interaction and concomitantly increased the ubiquitination of Bcr-Abl1 (Figure 4D). FRET assays also confirmed the loss of the interaction between Bcr-Abl1$_{Y852A}$ and PTP1B$_{WT}$ (Figure 4E,F).

Next, MST was conducted to evaluate the direct binding of SBF-1 and PTP1B. A robust binding curve was only observed in the GFP-PTP1B$_{WT}$ sample with a *Kd* at 23.2 ± 0.8 nM (Figure 5A). However, 80 nM of SBF-1 increased the stability of PTP1B$_{WT}$ protein to a significantly larger extent than PTP1B$_{Y46T}$ protein in CETSA (Figure 5B). As a control, there is no difference between the stability of PTP1B$_{WT}$ and PTP1B$_{K116R}$ (a random mutant control) protein in the presence of SBF-1 (Figure S3). When CETSA was performed to test the interaction of SBF-1 with Bcr-Abl1, SBF-1 shifted the Bcr-Abl1$_{WT}$ heat denaturation curve to a slightly higher temperature than Bcr-Abl1$_{\Delta PH}$ (Figure 5C). Similar results were obtained for the Bcr-Abl1$_{Y852A}$ heat denaturation curve (Figure 5D).

### 3.4 | The blockade of PTP1B-Bcr-Abl1 interaction promotes c-Cbl-mediated selective autophagic degradation of Bcr-Abl1

Increasing evidence indicates that c-Cbl, a ubiquitin E3 ligase, plays an essential role in the ubiquitin-dependent degradation of Bcr-Abl1.[14,20,21] In the presence of Y46T PTP1B mutant, the ubiquitination of Bcr-Abl1 was profoundly reduced by c-Cbl siRNA in HEK293 cells (Figure 6A) and silencing c-Cbl impaired Bcr-Abl1 degradation. In addition, c-Cbl siRNA markedly reduced SBF-1-induced Bcr-Abl1 degradation and its cytotoxicity in K562 cells (Figures 6B and S4). Since different types of poly-ubiquitination processes, including K48-, K63-,

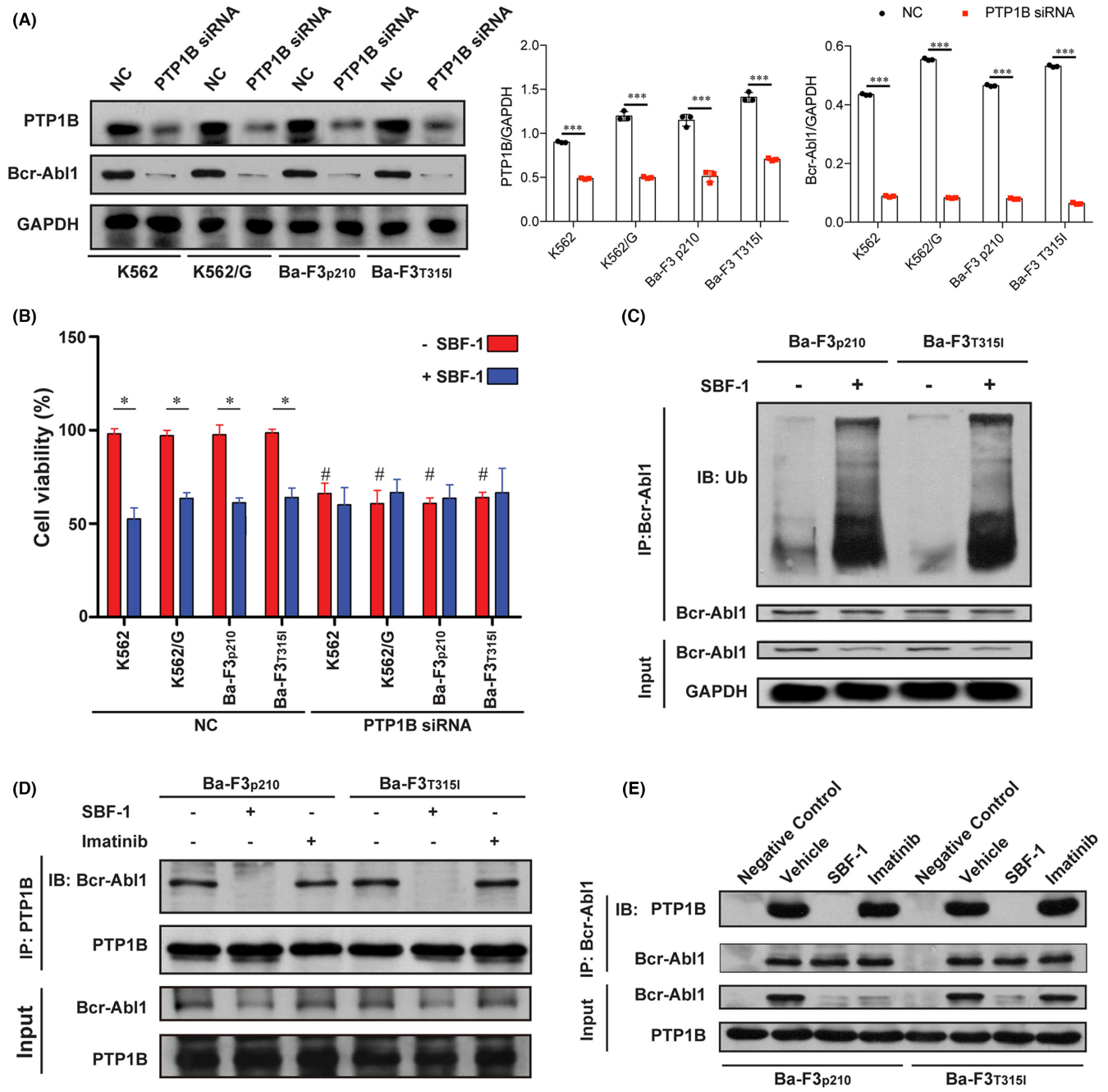


FIGURE 2 T315I mutant Bcr-Abl1 degradation by SBF-1 through disrupting the interaction between PTP1B and Bcr-Abl1. (A) The expression of PTP1B and Bcr-Abl1 was detected by western blot after knockdown of PTP1B. (B) Cell viability was determined by MTT assay after the transfected cells were treated with SBF-1 (40 nM) for 48 h. $^{\#}P<0.05$ versus the cells transfected with NC siRNA. (C) Co-IP analysis of the interaction between Bcr-Abl1 and ubiquitin (Ub). (D) Co-IP analysis of the interaction between PTP1B and Bcr-Abl1. (E) Immunoprecipitation showing the interaction between PTP1B and Bcr-Abl1 in the bone marrow samples from the intravenously transplanted model described in Figure 1C. $^{*}P<0.05$, $^{***}P<0.005$

and k27-linked ubiquitination, have been implicated to determine protein fate,[22,23] we set out to analyze which type of Bcr-Abl1 ubiquitination is mediated by c-Cbl. As shown in Figure 6C, SBF-1 treatment promoted K27-linked ubiquitination of Bcr-Abl1. Such K27-linked ubiquitination was reduced by c-Cbl silencing (Figure 6D) and an interaction between Bcr-Abl1 and c-Cbl was found in the case of the K27-linked ubiquitination. A previous study reported that a natural compound, oridonin, triggers chaperon-mediated proteasomal degradation of Bcr-Abl1 in leukemia.[24] Unlike SBF-1, oridonin treatment promoted K48-linked ubiquitination of Bcr-Abl1, which provides a universal signal for proteasomal degradation (Figure S5A,B). c-Cbl silencing showed no effect on oridonin-induced Bcr-Abl1 degradation (Figure S5C), and no interaction between Bcr-Abl1 and c-Cbl was found in the presence of oridonin (Figure S5D).

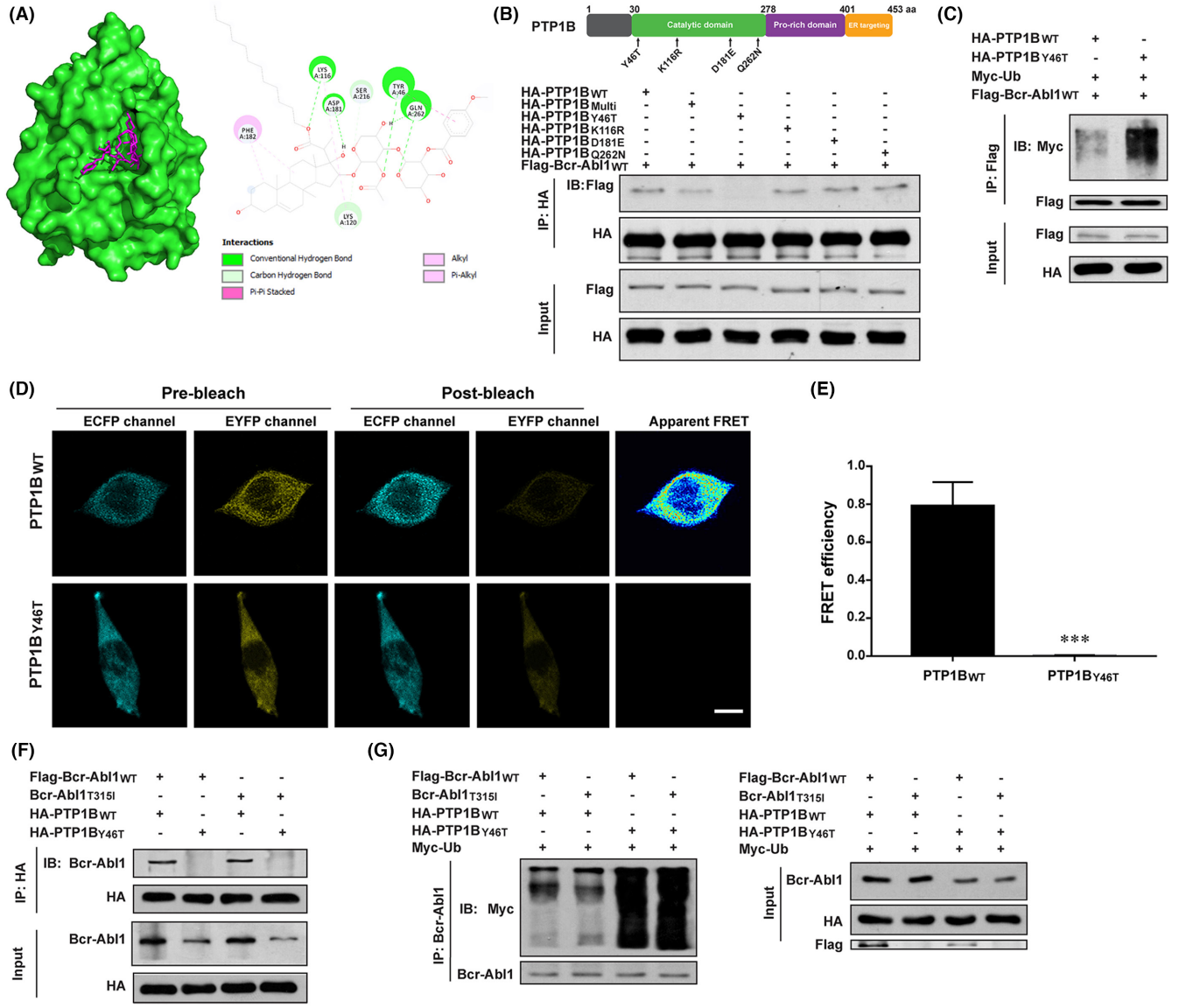


FIGURE 3 Tyr46 in PTP1B is crucial for the binding of Bcr-Abl1. (A) Molecular docking analysis of SBF-1 and PTP1B. (B) Co-IP analysis of the interaction between Flag-Bcr-Abl1$_{WT}$ and HA-PTP1B or its indicated mutants in transfected HEK293 cells. (C) Co-IP analysis of the interaction between Flag-Bcr-Abl1$_{WT}$ and Myc-Ub in the presence of HA-PTP1B$_{WT}$ or PTP1B$_{Y46T}$. (D) Visualization of FRET using acceptor photobleaching protocol. The ratio of the ECFP fluorescence intensity after photobleaching versus that before photobleaching depicted using discrete colors. Scale bar, 5 μm. (E) The mean FRET efficiency. ***$P < 0.005$. (F) Co-IP analysis of the interaction between HA-PTP1B$_{WT}$ or PTP1B$_{Y46T}$ and Flag-Bcr-Abl1$_{WT}$ or Bcr-Abl1$_{T315I}$. (G) Co-IP analysis of the interaction between Flag-Bcr-Abl1$_{WT}$ or Bcr-Abl1$_{T315I}$ and Myc-Ub in the presence of HA-PTP1B$_{WT}$ or PTP1B$_{Y46T}$

Next, we found that, apart from the proteasome inhibitor MG132, the autophagy inhibitors, including 3-MA, CQ, and Baf A1, inhibited the degradation of Bcr-Abl1 by SBF-1 in both Ba-F3p210 and Ba-F3T315I cells (Figure 6E). Such degradation was modestly reduced in K562 cells with ATG5 or Beclin 1 silencing (Figure S6A). Confocal microscopy showed that SBF-1, but not oridonin, increased the co-colocalization of Bcr-Abl1 and lysotracker (Figure S6B). Ubiquitin chains attached to the substrates serve as a major signal responsible for the recognition of cargo receptors, such as p62.[25,26] We observed that Bcr-Abl1 interacted with p62 after 12 h of SBF-1 treatment (Figure 6F), but not after oridonin treatment (Figure S6C). Notably, SBF-1 promoted the selective binding of p62 to Bcr-Abl1 with K27-linked ubiquitination, evidenced by reciprocal immunoprecipitation of Flag-Bcr-Abl1 and HA-K27 ubiquitin (Figures 6G and S6D). Such a binding was abolished by c-Cbl siRNA (Figure 6H).

### 3.5 | Dephosphorylation of Tyr1086 in the Bcr-Abl1 SH2 domain by PTP1B protects the recruitment of c-Cbl to Bcr-Abl1

Given that c-Cbl frequently recognizes phosphorylated tyrosine on activated tyrosine kinases and PTP1B is protein tyrosine phosphatase,[27,28] we hypothesized that the blockade of PTP1B-Bcr-Abl1

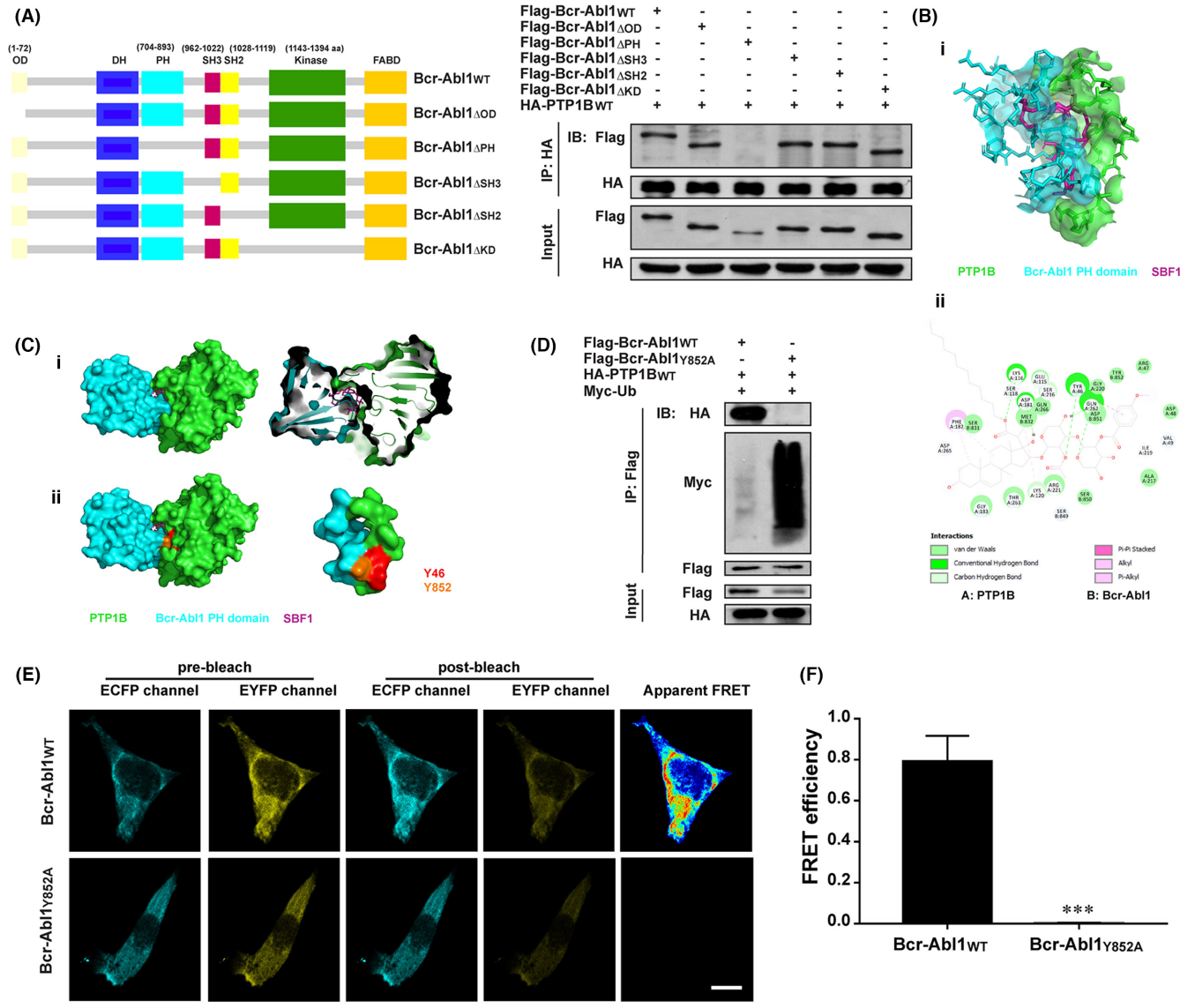


FIGURE 4 Tyr852 in the Bcr-Abl1 PH domain is crucial for the binding of PTP1B. (A) Co-IP analysis of the interaction between HA-PTP1B$_{WT}$ and Flag-Bcr-Abl1$_{WT}$ or its indicated truncation mutants in transfected HEK293 cells. (B) Computer modeling for the PTP1B-SBF-1-Bcr-Abl1 PH domain complex. General (i) and detailed (ii) views of the interactions among the triple complex. (C) A predicted binding site of SBF-1 that targets PTP1B and the Bcr-Abl1 PH domain. (i) The scenario showing the binding of SBF-1 to the interface between PTP1B and the Bcr-Abl1 PH domain, and (ii) the critical amino acid residues for the interaction marked in red (Y46) and orange (Y852). (D) Co-IP analysis of the interaction between Flag-Bcr-Abl1$_{WT}$ or Bcr-Abl1$_{Y862A}$ and Myc-Ub in the presence of HA-PTP1B$_{WT}$. (E) Visualization of FRET using acceptor photobleaching protocol. Scale bar, 5 μm. (F) The mean FRET efficiency. ***$P < 0.005$

interaction might enhance the tyrosine phosphorylation levels of critical residues within Bcr-Abl1, which would promote c-Cbl recruitment and lead to Bcr-Abl1 degradation. Using phos-tag gel electrophoresis, we observed that SBF-1 treatment increased the phosphorylation of endogenous Bcr-Abl1 in K562 cells, reaching a peak after 12 h (Figure 7A). Furthermore, we performed mass spectrometry analysis for the phosphorylated Bcr-Abl1 enriched by immunoprecipitation using anti-c-Abl antibody, and compared the differential changes in the phosphorylation levels of several residues within Bcr-Abl1 before and after SBF-1 treatment. The tyrosine 1086 in the Bcr-Abl1 SH2 domain was identified as the only tyrosine (Figure S7). The Y1086A mutation modestly impaired the phosphorylation of exogenous Bcr-Abl1 induced by SBF-1 (Figure 7B). In addition, immunoprecipitation analysis confirmed that the Y1086A mutation decreased the tyrosine phosphorylation of Bcr-Abl1, which was induced by SBF-1 (Figure 7C). The interaction between Bcr-Abl1$_{WT}$ and c-Cbl was enhanced after SBF-1 treatment, but was abolished by the Y1086A mutation. Correspondingly, the ubiquitination of Bcr-Abl1 and its binding with p62 induced by SBF-1 were almost abrogated in the cells with Bcr-Abl1$_{Y1086A}$ mutant (Figure 7D). To further confirm the role of PTP1B phosphatase in the process of c-Cbl recruitment,

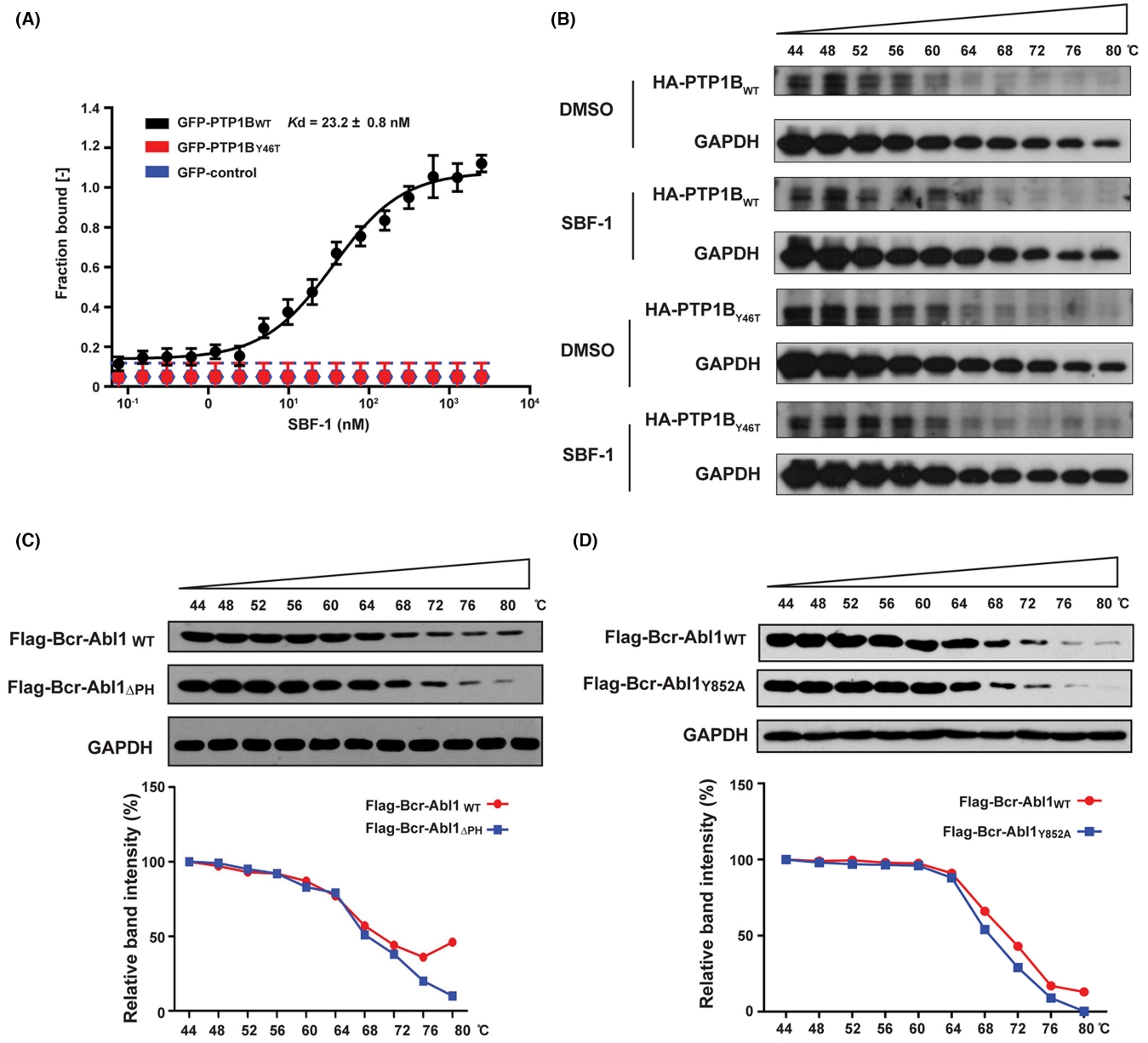


FIGURE 5 SBF-1 preferentially binds to PTP1B at Tyr46 site. (A) MST analysis of SBF-1 binding to GFP-PTP1B$_{WT}$, GFP-PTP1B$_{Y46T}$ or free GFP in HEK293 cell lysates. (B) The stabilizing effect of SBF-1 for PTP1B$_{WT}$ and PTP1B$_{Y46T}$ at increasing temperature up to 80°C in HEK293 cells. Cell lysates were determined by western blot. (C) The stabilizing effect of SBF-1 for Bcr-Abl1$_{WT}$ and Bcr-Abl1$_{\Delta PH.}$ (D) The stabilizing effect of SBF-1 for Bcr-Abl1$_{WT}$ and Bcr-Abl1$_{Y852A}$. CETSA samples were determined by western blot

we silenced PTP1B with siRNA. As expected, silencing PTP1B increased the phosphorylation of Bcr-Abl1 in the cells transfected with Bcr-Abl1$_{WT}$ (Figure 7E). The level of Bcr-Abl1 phosphorylation increased to a lesser extent in the cells transfected with Bcr-Abl1$_{Y1086A}$. Similar to our findings in SBF-1-treated cells, the Y1086A mutation decreased the tyrosine phosphorylation of Bcr-Abl1 and abolished the interaction of Bcr-Abl1 with c-Cbl in cells with PTP1B silencing (Figure 7F). The ubiquitination of Bcr-Abl1 and its binding with p62 were also reduced by the Y1086A mutation (Figure 7G). Taken together, the blockade of the PTP1B-Bcr-Abl1 interaction is crucial for autophagy-mediated Bcr-Abl1 degradation (Figure 7H).

## 4 | DISCUSSION

In this study, we observed the comparably robust growth inhibition for SBF-1 in CML cells harboring either native or T315I mutant Bcr-Abl1 in vitro and in vivo, which was accompanied by the degradation of Bcr-Abl1 protein. Apart from the blockade of the interaction between PTP1B and native Bcr-Abl1 in our previous finding,[15] SBF-1 also disrupted the interaction between PTP1B and T315I mutant Bcr-Abl1, suggesting that interrupting the PTP1B-Bcr-Abl1 interaction is potential to trigger the degradation of both native and mutant Bcr-Abl1. Utilizing SBF-1 as a tool, we found that Tyr46 in the PTP1B catalytic domain and Tyr852 in the Bcr-Abl1 PH domain are

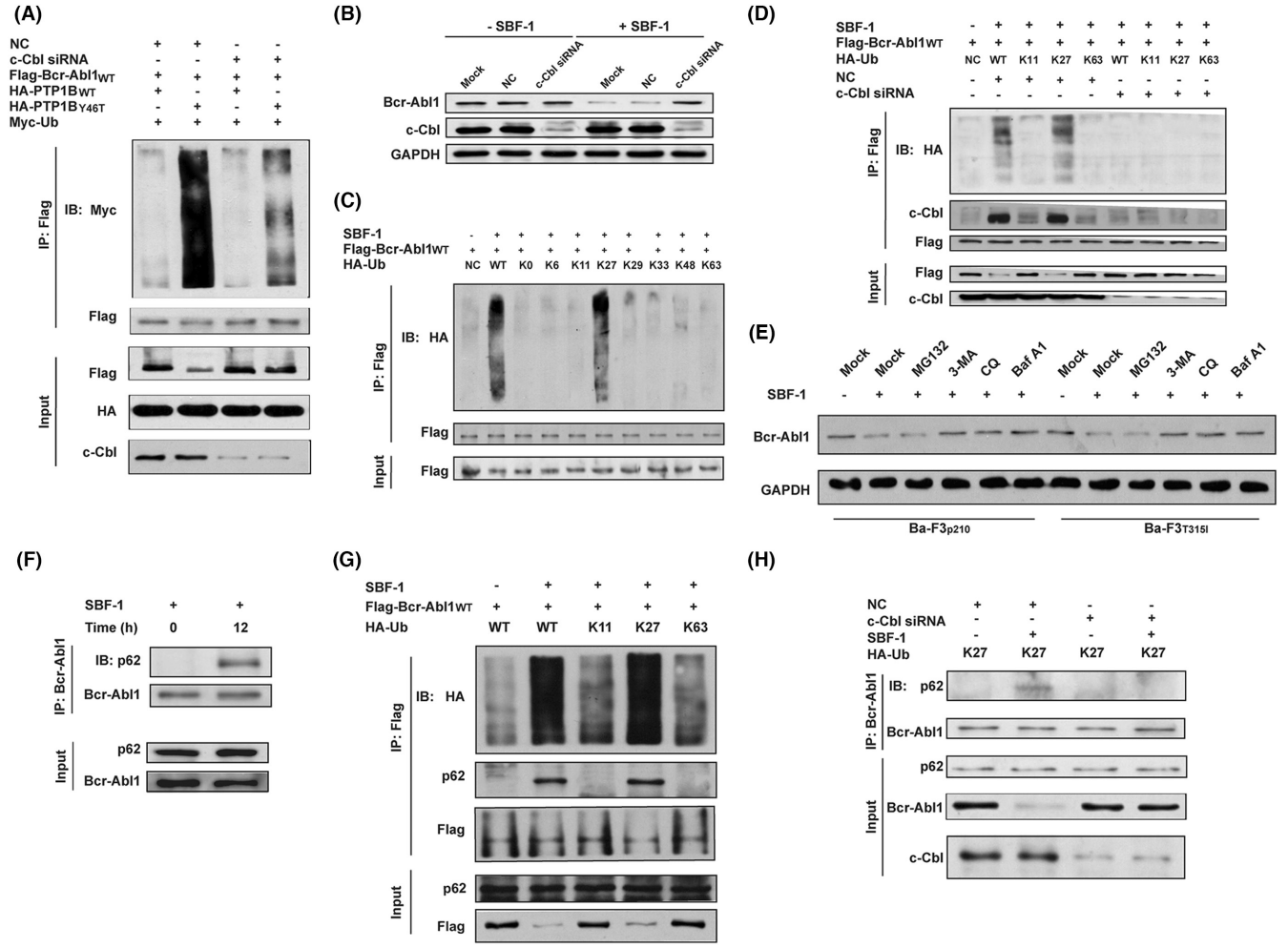


**FIGURE 6** Blockade of the PTP1B-Bcr-Ab interaction promotes the autophagic degradation of Bcr-Abl1. (A) Co-IP analysis of the interaction between Flag-Bcr-Abl1$_{WT}$ and Myc-Ub in transfected HEK293 cells. (B) K562 cells were transfected with scramble siRNA or c-Cbl siRNA and then treated with or without SBF-1 (40 nM) for 48 h. The lysates were analyzed with indicated antibodies by western blot. (C) Co-IP analysis of the interaction between Flag-Bcr-Abl1$_{WT}$ and HA-Ub or its indicated mutants in transfected HEK293 cells. (D) Co-IP analysis of the interaction between Flag-Bcr-Abl1$_{WT}$ and HA-Ub or its indicated mutants in transfected HEK293 cells with or without c-Cbl knockdown. (E) Ba-F3p210 or Ba-F3T315I cells were pre-treated with 3-MA, CQ, or Baf A1 for 2 h and then treated with or without SBF-1. The expression of Bcr-Abl1 was detected by western blot. (F) Co-IP analysis of the interaction between Bcr-Abl1 and p62 in K562 cells treated with or without SBF-1 for indicated time points. (G) HEK293 cells were transfected with Flag-Bcr-Abl1$_{WT}$ and HA-Ub or its indicated mutants and then treated with or without SBF-1. Co-IP analysis of the interaction between Flag-Bcr-Abl1 and the indicated proteins. (H) Co-IP analysis of the interaction between Bcr-Abl1 and p62 in the transfected K562 cells with or without c-Cbl knockdown

critical for their interaction. SBF-1 preferentially binds to PTP1B at the Tyr46 site. Moreover, the phosphorylation of Tyr1086 within the Bcr-Abl1 SH2 domain recruits the E3 ubiquitin ligase c-Cbl to catalyze K27-linked ubiquitin chains, which serve as a recognition signal for p62-dependent autophagic degradation. Dephosphorylation of Bcr-Abl1 at Tyr1086 by PTP1B prevents the recruitment of c-Cbl and in turn enhances Bcr-Abl1 protein stability. Expanding our previous finding,[15] this study further demonstrates the power of SBF-1-mediated blockade of the PTP1B-Bcr-Abl1 interaction as a potential therapeutic approach in TKI-resistant CML with point mutations.

As a large fusion protein, Bcr-Abl1 features multiple domains.[29] In addition to the tyrosine kinase domain, many other domains act as a protein-interaction scaffold in leukemogenic signaling. For example, the SH2 domain interacts SHC and results in the recruitment of GRB2, which contributes to the activation of the RAS pathway.[30] The PH domain is commonly involved in targeting proteins to membrane by binding phosphatidylinositol-phosphate.[31] Recent studies have reported that the tyrosine phosphatase Ubash3b/Sts1 interacts with the PH domain in p210 Bcr-Abl1 and influences the p210 signaling network.[31,32] This study is the first to demonstrate that the tyrosine phosphatase PTP1B interacts with the PH domain to stabilize p210 Bcr-Abl1. In our predicted scenario of the complex, both Tyr46 in PTP1B and Tyr852 in Bcr-Abl1 PH domain are crucial for their interaction, as proved by mutation experiments. Targeting the PTP1B-Bcr-Abl1 interaction to induce p210 Bcr-Abl1 protein degradation is not limited when mutations occur within its kinase domain, which accounts for the inhibition of SBF-1 on CML cells harboring either native or T315I mutant Bcr-Abl1. Thus, the

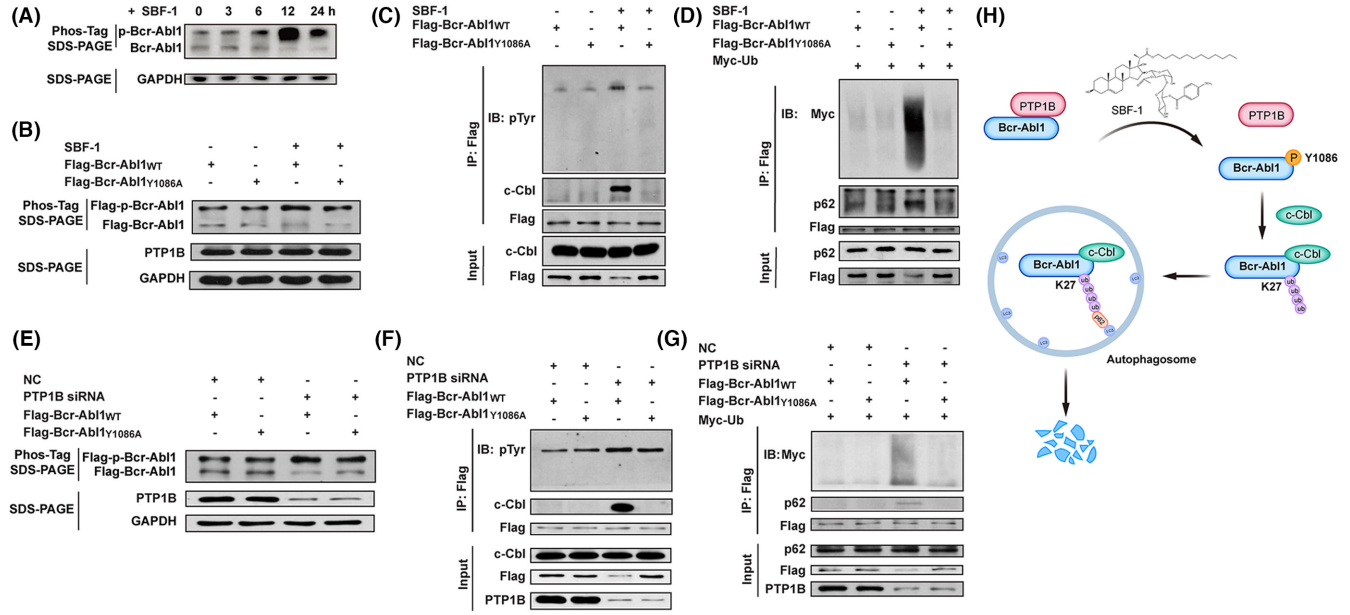


**FIGURE 7** The phosphorylation of Tyr1082 within the SH2 domain of Bcr-Abl1 is required for the recruitment of c-Cbl. (A) K562 cells were treated with SBF-1 for the indicated time points. (B) HEK293 cells transfected with Flag-Bcr-Abl1$_{WT}$ or Bcr-Abl1$_{Y1086A}$ were treated with SBF-1 (40 nM) for 12 h. Cell lysates were subjected to Phos-tag gel electrophoresis and immunoblotted with the indicated antibodies. (C and D) Co-IP analysis of the interaction between Flag-Bcr-Abl1 and the indicated proteins in transfected HEK293 cells. (E) HEK293 cells were transfected with Flag-Bcr-Abl1$_{WT}$ or Bcr-Abl1$_{Y1086A}$ along with PTP1B siRNA. Cell lysates were subjected to Phos-tag gel electrophoresis and immunoblotted. (F and G) Co-IP analysis of the interaction between Flag-Bcr-Abl1 and the indicated proteins in transfected HEK293 cells. (H) A schematic model for the role of the blockade of the PTP1B-Bcr-Abl1 interaction in regulating Bcr-Abl1 stability

PTP1B-Bcr-Abl1 interaction might be one of druggable vulnerabilities of TKI-resistant CML.

In line with a previous finding[21] in which the SH2 domain of Bcr-Abl1 is the direct binding site of c-Cbl, this study demonstrates that c-Cbl bound to phosphorylated Tyr1086 within the Bcr-Abl1 SH2 domain and the phosphorylation level of Tyr1086 was regulated by PTP1B. When the binding of PTP1B to Bcr-Abl1 was disrupted or PTP1B was silenced, the increase in the level of phosphorylated Bcr-Abl1 was impaired by the Y1086A mutation. Given that c-Cbl is known to mediate the ubiquitin-dependent degradation of Bcr-Abl1, the stability of Bcr-Abl1 could depend on the phosphorylation level of Tyr1086. Indeed, the Y1086A mutation abolished the interaction of Bcr-Abl1 with c-Cbl and inhibited the degradation of Bcr-Abl1 protein in the presence of SBF-1 or PTP1B siRNA.

In conclusion, this study unravels the action mechanism of PTP1B in stabilizing Bcr-Abl1 protein, realizes a specific degradation of T315I mutant Bcr-Abl1 protein, and opens up interesting perspectives for small molecular degraders of Bcr-Abl1 in therapeutic settings.

## DISCLOSURE

The authors have declared no conflict of interest for this article.

## ETHICAL APPROVAL

The research protocols were approved by an Institutional Reviewer Board and the Animal Ethical and Welfare Committee of Nanjing University. The registration no. of this animal study/trial is IACUC-D2102006.

## ACKNOWLEDGMENTS

We would like to thank Professor Yijun Chen and Professor Xia Li for their kind donation of cells and plasmids.

## FUNDING INFORMATION

National Natural Science Foundation of China, Grant/Award Numbers 21937005 and 81974504, and Natural Science Foundation of Jiangsu Province Grant/Award Numbers BK20191251 and BK20210184.

## ORCID

*Yan Shen* https://orcid.org/0000-0002-3204-7095

## REFERENCES

1. Deininger MW, Goldman JM, Melo JV. The molecular biology of chronic myeloid leukemia. *Blood*. 2000;96:3343-3356.
2. Chen J, Yu WM, Daino H, Broxmeyer HE, Druker BJ, Qu CK. SHP-2 phosphatase is required for hematopoietic cell transformation by Bcr-Abl1. *Blood*. 2007;109:778-785.
3. Helgason GV, Karvela M, Holyoake TL. Kill one bird with two stones: potential efficacy of BCR-ABL1 and autophagy inhibition in CML. *Blood*. 2011;118:2035-2043.
4. Hochhaus A, Larson RA, Guilhot F, et al. Long-term outcomes of imatinib treatment for chronic myeloid leukemia. *N Engl J Med*. 2017;376:917-927.

5. Hantschel O, Grebien F, Superti-Furga G. The growing arsenal of ATP-competitive and allosteric inhibitors of BCR-ABL1. *Cancer Res*. 2012;72:4890-4895.
6. Soverini S, Colarossi S, Gnani A, et al. Contribution of ABL kinase domain mutations to imatinib resistance in different subsets of Philadelphia-positive patients: by the GIMEMA working party on chronic myeloid leukemia. *Clin Cancer Res*. 2006;12:7374-7379.
7. Druker BJ, Guilhot F, O'Brien SG, et al. Five-year follow-up of patients receiving imatinib for chronic myeloid leukemia. *N Engl J Med*. 2006;355:2408-2417.
8. Zabriskie MS, Eide CA, Tantravahi SK, et al. BCR-ABL11 compound mutations combining key kinase domain positions confer clinical resistance to ponatinib in Ph chromosome-positive leukemia. *Cancer Cell*. 2014;26:428-442.
9. Lai AC, Toure M, Hellerschmied D, et al. Modular PROTAC design for the degradation of oncogenic BCR-ABL1. *Angew Chem Int Ed Engl*. 2016;55:807-810.
10. Shibata N, Miyamoto N, Nagai K, et al. Development of protein degradation inducers of oncogenic BCR-ABL1 protein by conjugation of ABL kinase inhibitors and IAP ligands. *Cancer Sci*. 2017;108:1657-1666.
11. Burslem GM, Schultz AR, Bondeson DP, et al. Targeting BCR-ABL11 in chronic myeloid leukemia by PROTAC-mediated targeted protein degradation. *Cancer Res*. 2019;79:4744-4753.
12. Shibata N, Shimokawa K, Nagai K, et al. Pharmacological difference between degrader and inhibitor against oncogenic BCR-ABL1 kinase. *Sci Rep*. 2018;8:13549.
13. Cromm PM, Crews CM. Targeted protein degradation: from chemical biology to drug discovery. *Cell Chem Biol*. 2017;24:1181-1190.
14. Alvira D, Naughton R, Bhatt L, Tedesco S, Landry WD, Cotter TG. Inhibition of protein-tyrosine phosphatase 1B (PTP1B) mediates ubiquitination and degradation of Bcr-Abl1 protein. *J Biol Chem*. 2011;286:32313-32323.
15. Elgehama A, Chen W, Pang J, et al. Blockade of the interaction between Bcr-Abl1 and PTB1B by small molecule SBF-1 to overcome imatinib-resistance of chronic myeloid leukemia cells. *Cancer Lett*. 2016;372:82-88.
16. Shi B, Wu H, Yu B, Wu J. 23-oxa-analogues of OSW-1: efficient synthesis and extremely potent antitumor activity. *Angew Chem*. 2004;43:4324-4327.
17. Gao J, Fan M, Xiang G, et al. Diptoindonesin G promotes ERK-mediated nuclear translocation of p-STAT1 (Ser727) and cell differentiation in AML cells. *Cell Death Dis*. 2017;8:e2765.
18. Qu Y, Gharbi N, Yuan X, et al. Axitinib blocks Wnt/beta-catenin signaling and directs asymmetric cell division in cancer. *Proc Natl Acad Sci USA*. 2016;113:9339-9344.
19. Jafari R, Almqvist H, Axelsson H, et al. The cellular thermal shift assay for evaluating drug target interactions in cells. *Nat Protoc*. 2014;9:2100-2122.
20. Mao JH, Sun XY, Liu JX, et al. As4S4 targets RING-type E3 ligase c-CBL to induce degradation of BCR-ABL1 in chronic myelogenous leukemia. *Proc Natl Acad Sci USA*. 2010;107:21683-21688.
21. Bhat A, Kolibaba K, Oda T, Ohno-Jones S, Heaney C, Druker BJ. Interactions of CBL with BCR-ABL1 and CRKL in BCR-ABL1-transformed myeloid cells. *J Biol Chem*. 1997;272:16170-16175.
22. Fushman D, Walker O. Exploring the linkage dependence of polyubiquitin conformations using molecular modeling. *J Mol Biol*. 2010;395:803-814.
23. Jin S, Tian S, Luo M, et al. Tetherin suppresses type I interferon signaling by targeting MAVS for NDP52-mediated selective autophagic degradation in human cells. *Mol Cell*. 2017;68:308-322.e304.
24. Huang H, Weng H, Dong B, Zhao P, Zhou H, Qu L. Oridonin triggers chaperon-mediated proteasomal degradation of BCR-ABL1 in leukemia. *Sci Rep*. 2017;7:41525.
25. Kraft C, Peter M, Hofmann K. Selective autophagy: ubiquitin-mediated recognition and beyond. *Nat Cell Biol*. 2010;12:836-841.
26. Komander D, Rape M. The ubiquitin code. *Annu Rev Biochem*. 2012;81:203-229.
27. Yip SC, Saha S, Chernoff J. PTP1B: a double agent in metabolism and oncogenesis. *Trends Biochem Sci*. 2010;35:442-449.
28. Thien CB, Langdon WY. Cbl: many adaptations to regulate protein tyrosine kinases. *Nat Rev Mol Cell Biol*. 2001;2:294-307.
29. Ren R. Mechanisms of BCR-ABL1 in the pathogenesis of chronic myelogenous leukaemia. *Nat Rev Cancer*. 2005;5:172-183.
30. Goga A, McLaughlin J, Afar DE, Saffran DC, Witte ON. Alternative signals to RAS for hematopoietic transformation by the BCR-ABL1 oncogene. *Cell*. 1995;82:981-988.
31. Reckel S, Gehin C, Tardivon D, et al. Structural and functional dissection of the DH and PH domains of oncogenic Bcr-Abl1 tyrosine kinase. *Nat Commun*. 2017;8:2101.
32. Reckel S, Hamelin R, Georgeon S, et al. Differential signaling networks of Bcr-Abl1 p210 and p190 kinases in leukemia cells defined by functional proteomics. *Leukemia*. 2017;31:1502-1512.


## SUPPORTING INFORMATION

Additional supporting information can be found online in the Supporting Information section at the end of this article.

**How to cite this article:** Elgehama A, Wang Y, Yu Y, et al. Targeting the PTP1B-Bcr-Abl1 interaction for the degradation of T315I mutant Bcr-Abl1 in chronic myeloid leukemia. *Cancer Sci*. 2023;114:247-258. doi: 10.1111/cas.15580